Int. J. Environ. Res. Public Health **2008**, *5(1)*, 12-25

International Journal of
Environmental Research and Public Health
ISSN 1661-7827
www.ijerph.org

Cytotoxic Responses and Potential Respiratory Health Effects of Carbon and Carbonaceous Nanoparticulates in the Paso del Norte Airshed Environment

K. F. Soto[1,2], L. E. Murr[1*] and K. M. Garza[3]

[1]Department of Metallurgical and Materials Engineering, the University of Texas at El Paso, El Paso, TX 79968 USA
[2]Lockheed Martin Aeronautics Company, Fort Worth, TX 76101, USA
[3]Department of Biological Sciences, The University of Texas at El Paso, El Paso, TX 79968, USA
*Correspondence to Dr. L. E Murr: Email: lemurr@utep.edu

Received: 30 October 2007 / Accepted: 29 February 2008 / Published: 30 March 2008

Abstract: We have utilized a range of manufactured or commercial nanoparticulate materials, including surrogate carbon nano-PM along with combustion-generated carbonaceous (soot) nano-PM characteristic of environmental nano-PM (both indoor and outdoor) to investigate and compare their cytotoxic response *in vitro* with an immortalized human epithelial (lung model) cell line (A549). These have included nano-Ag, Al_2O_3, TiO_2, Fe_2O_3, ZrO_2, Si_3N_4, chrysotile asbestos, BC, 2 types of MWCNT-aggregate PM (MWCNT-R and MWCNT-N), and high-volume glass fiber collected soots: candle, wood, diesel (truck), tire, and 3-types of natural gas kitchen burner-generated soots: yellow (fuel-rich) flame, low-flow blue flame, and normal flow blue flame soot PM. These carbonaceous nano-PM species can be found in either the indoor and outdoor environments or microenvironments. Two-day and two-week *in-vitro* cultures of A549 showed cell death (or decreased cell viability) for all nanoparticulate materials, but especially significant for all but the TiO_2 and candle, wood, and diesel PM. The natural gas kitchen burner combustion PM cell death response was characteristic of BC and MWCNT PM. There was no correlation with total PAH content of the soot PM. Cytokine release (IL-6, IL-8) was detected for the Ag, Fe_2O_3, asbestos, BC and the MWCNT PM. Reactive oxygen species (ROS) production was also detected for Ag, Fe_2O_3, ZrO_2, asbestos, BC, and the MWCNT aggregate PM, as well as the natural gas kitchen burner combustion PM. TEM, FESEM, and optical microscopy examination of these nanomaterials illustrate the wide range in PM morphologies and crystallinities as well as cell morphologies. Taken together, these results illustrate proinflammatory and related respiratory health issues in relation to environmental nanoparticulates.

Keywords: Cytotoxicity, IL-6, IL-8, ROS, multiwall carbon nanotubes, soot nano-PM, TEM

Introduction

It is now quite apparent that nanoparticulate materials of virtually all types (morphologies, chemistries, crystal structures, crystallinity variations, etc.) pose a variety of health hazards, particularly respiratory hazards. This includes a variety of natural (mineral or geologic), manufactured, and other anthropogenic nanoparticulate materials in the ambient and microenvironments, as well as a variety of occupational environments [1-17]. Both *in vivo* and *in vitro* assays have provided information on common biological exposure responses, although it remains unclear what biomaterials or nanomaterials properties or physicochemical parameters are specifically related to this biological activity either individually or collectively. In addition, it is often unclear whether *in vitro* assays over the short term (2 days to 2 weeks) can sensibly predict *in vivo* response, especially since animal models are themselves inconsistent and do not always predict human responses because of the inherent variations in the specific state of health and exposure tolerance. Correspondingly, *in vitro* assays are more controlled than *in vivo* studies and can provide rapid and potential assessments of health effects. Human cell cultures

eliminate, to some extent, the complexity and variability of human metabolisms and biochemical phenomena. Both *in vitro* and *in vivo* assays assess acute exposure and not chronic exposure to nanomateirals, and while *in vitro* assays demonstrate the ability to compare relative toxicities in terms of cell viability or cell death over short time periods, standardized dosing protocols are not well established, and the interconversion to ambient environmental nanoparticulate concentrations (either particle concentrations or mass concentrations) are nonexistent. In addition, there is the question of how effectively short term assay results can predict, or even suggest, potential, longer-term health effects; particularly serious diseases involving mutagenicity and carcinogenicity.

In addition to *in vitro* cell viability or cell death assays using MTT-based optical densitometry, or cytokine Enzyme Linked Immuno Sorbent Assay (ELISA) studies which measure the up-regulation and release of interlekins by the cells, and measurement of reactive oxygen species (ROS) production in response to cellular insults can provide a range of markers of inflammatory of inflammatory response. Cytokines are soluble peptides involved in a range of signal transduction pathways which regulate cell differentiation, growth, and cell death; cytokines also recruit neutrophils, macrophages, and other mobile-immune cells to specific sites of injury or insult [18-20]. Many recent ELISA studies have utilized the immortalized A549 human epithelial lung cell line which provides an effective *in vitro* lung cell model. Interleukin-6 (IL-6) and IL-8 have been studied as markers of inflammatory response both in the A549 cell culture models, and in bronchial alveolar laverage fluid of animals [21-27], providing a biomarker link between *in vitro* and *in vivo* studies. IL-6 has been linked to allergic responses involving asthma, while IL-8 has been associated with chronic obstructive pulmonary disease (COPD) [28]. A large body of research has examined the role of ultrafine or nanoparticulate matter in exacerbations of COPD in particular [13].

Inflammatory response as well as longer-term chronic disease has been historically predicated upon the generation of reactive oxygen species (ROS). This has been true for respiratory and asthma-related phenomena and COPD, as well as the production of fibrosis, lung lesions, cancer, etc. [2, 5, 29-32]. Nel, et la. [33] have proposed that ROS generation and oxidative stress is the "best developed paradigm to explain the toxic effects of inhaled nanoparticles". These ROS include superoxide ($^{\bullet}O_2^-$), hydrogen peroxide, H_2O_2 (HOOH), and hydroxyol radical ($^{\bullet}$OH); which is one of the strongest biological oxidizing radicals [34]. Jung, et al. [35] recently found that $^{\bullet}$OH is formed by flame soot particles (FSP), black carbon (BC), and fine ambient particles ($PM_{2.5}$) in surrogate lung fluid where the mass-normalized $^{\bullet}$OH generation for FPS was ten times that for BC. Lung cells normally generate ROS concentrations easily neutralized by antioxidant defenses such as glutathione (GSH) and other antioxidant enzymes [36]. If nanoparticulates in the lungs produce excess ROS, then these defenses can be overwhelmed. Oxidative stress results when the GSH is depleted while the oxidized GSH accumulates. This results in airway inflammation and interstitial fibrosis. While somewhat controversial, Polansky [37] has described exogenous events that move a biological system from "good health" to "hronic disease" as a microcompetition with foreign DNA, characterized by excessive oxidative stress.

Nel, et al. [33] have recently suggested that *in vitro* assays of cell death and inflammatory biomarker cytokines along with ROS analysis and appropriate characterization, can serve as an example of a predictive paradigm for toxicity screening of nanoparticulate materials. In this study, we have implemented this analytical strategy to examine the toxicity, especially the comparative cytotoxicities, for a range of manufactured nanoparticulate materials, including carbon-based and carbonaceous materials, along with a range of anthropogenic, carbonaceous nanoparticulate materials, especially combustion-generated soots. These nanoparticulate materials have been carefully characterized, either in this study or in previous research, utilizing field-emission scanning electron microscopy (FESEM), and/or conventional transmission electron microscopy (CTEM) and scanning transmission electron microscopy (STEM) [38].

Experimental Methods and Materials

We have previously characterized and assayed a wide range of manufactured nanoparticulate materials [39]. More recently we have compared viability assays for these nanoparticulate materials for a murine macrophage cell line (RAW 264.7), a human alveolar macrophage cell line (THB-1), and a human general epithelial cell line (A549); illustrating that these cell lines each represent very similar if not identical cell viabilities (or cell death data) in the presence of the nanocarbon material relative to controls, calculated by absorbance at 570 nm, for exposure times ranging from 48 hrs (2 days) to 336 hrs (2 weeks) [12, 40, 41]. In addition, we have also developed a new assay for measuring the relative viability for human epithelial (A549) cells in culture exposed to a wide range of carbonaceous (soot) nanoparticulate materials, including candle soot or candle particulate matter (CPM), diesel particulate matter (DPM), wood particulate matter (WPM), tire particulate matter (TPM), and a variety of kitchen (natural gas) burner combustion nanoparticulates; which can include aggregates of multiwall carbon nanotubes and other multiconcentric fullerenes [41-43]. These soot nanoparticulate materials were collected on high-volume air-flow glass fiber filters which were placed in contact with the human epithelial cells (A549) in large flat-well arrays [41, 42]. In this study, we utilized these same nanoparticulate materials (both manufactured and anthropogenic/combustion-generated) to

provide a broad comparative assessment of cytotoxicity and release of proinflammatory cytokines, as well as the production of ROS, in the widely used *in vitro* lung cell line model A549 human epithelial cells [7, 24]. Correspondingly, we compared the variation in these phenomena as a means to assess the potential health hazards for these nanoparticulate materials in the ambient air as well as specific micro-environments, including occupational environments.

Viability/Cell Death Analysis

We assessed A549 human epithelial cell death (as a percentage of dead or non-viable cells) using a high-affinity nucleic acid fluorescent strain (Sytox: Molecular Probe, Eugene, OR) that penetrates compromised cell membranes, but not the membranes of viable cells. The A549 cells were cultured in 6-well plates at 3 x 10^6 cells per well. As controls, the cells remained untreated (media only) or were given the vehicle control (dimethyl sulfoxide – DMSO) as described in detail elsewhere [12, 15, 39, 41]. The cells were treated with manufactured nanomaterials diluted in DMSO. The nanomaterials included: commercial black carbon (BC), on arc evaporation-grown multiwall carbon nanotube aggregate material (MWCNT-R), A Ni-catalyst-grown multiwall carbon nanotube material (MWCNT-N), Fe_2O_3, ZrO_2, Al_2O_3, Si_3N_4, Ag, TiO_2 (rutile and anatase forms), and mineral (chrysotile) asbestos ($Mg_3Si_2O_5$ $(OH)_4$). The cells were treated with 5 μg/mL of material for 48 h (an acute exposure) or with 0.5 μg/mL of material (a non-cytotoxic concentration for 48 h) for 336 h (a relative chronic exposure). For the 336 h treatment, all wells had 80% of the media removed and were given fresh media (with or without the nanocarbon materials at 5 μg/mL) every 48 hrs, so as to provide a continuous nutrition source and a relatively constant concentration of the nanocarbon materials. Following the treatment period, all media was removed, the cells were trypsinized (0.250% trypsin), and were resuspended in a 3% protein-containing PBS buffer. The cells were then treated with Sytox (10 nM) for 20 min. at 37°C. Afterwards, the cells were analyzed by flow cytometry (FC500 flow cytometer by Beckman Coulter). To determine the percentage of Sytox-positive cells, i.e., those exhibiting cell death, a total of 10,000 events were assessed per sample using the CXP Software. After 48 h and 336 h after incubation in 96-well plate arrays, media was removed, trypsinized, and resuspended in medium before addition of Sytox (10 nM) for 20 minutes at 37°C. The cells were then analyzed using fluorescence-activated cell sorter (FACS) to determine the percentage of Sytox-positive cells, i.e., those exhibiting cell death.

Cytokine ELISA Analysis

We determined the concentrations of IL-6 and IL-8 in A549 cell culture media supernatants using sandwich enzyme-linked immunosorbent assays (ELISA). The supernatants were collected after 48 h viability assays for the manufactured nanoparticulate materials and the filter-collected carbonaceous nanoparticulate materials described in detail elsewhere [39, 41]. The microtiter ELISA plates were coated over night with capture antibody and incubated at 40ºC Plates were blocked at room temperature with 3% bovine serum albumin in PBS for 2-3 hours. After washing, the samples were added in duplicate and incubated for 2 hours at room temperature. The plates were later incubated with biotin conjugated anti-cytokine antibody and were subsequently incubated with horseradish peroxidase-labeled avidin (Vector Laboratories). The enzyme substrate O-phenylenediamine (Sigma) was utilized for color development. Cytokine concentration was calculated against human recombinant cytokines using the BD pharmigen cytokine detection kits.

ROS Analysis

To determine the production of ROS, the A549 cells were grown in 96-well, flat-bottomed plates (50,000 cells per well) in the presence or absence of the manufactured nanoparticulate or nanocarbon materials (along with a DMSO vehicle control). Following a 48 h incubation, media was removed, the cells were washed with PBS, and were loaded with 10 μM DCF-DA (2,7-dichlorofluorescein diacetate) in PBS containing 25 mM HEPES, for 30 min. at 37°C. DCF-DA is a cell-permeant indictor for reactive oxygen species that is nonfluorescent until the acetate groups are removed by intracellular esterases and oxidation occurs within the cell. The cells were then washed twice and fluorescence intensity was determined at 485 nm excitation and 590 nm emissions, using an automated fluorescence reader (Fluorocount, Hewlett-Packard Instrument, IL). Cultures in media and DMSO were included and 600 μM H_2O_2 was added to serve as an ROS reference for the media.

Nanoparticulate Materials Characterization

We examined the nano and microstructures as well as the crystallinity and crystal-structure details of all of the nanoparticulate materials tested using a variety of collection substrates amenable to either scanning electron microscopy, transmission electron microscopy, or both. The manufactured nanoparticulate materials were placed between silicon monoxide/formvar-coated 200 mesh Ni grids for observation in the TEM. Carbonaceous (soot) nanoparticulates were either collected upon these grids using thermophoretic precipitation [44,45] for TEM analysis, scrapped from filter collections onto the coated grid (sandwiches) for TEM, or observed directly on collection filters (either Ir sputter-coated or uncoated) in the SEM [38,42]. The SEM was a Hitachi S-4800 field-emission (FE) SEM. Samples were normally observed at low voltage to avoid charging and enhance resolution, either coated with ~4 nm Ir, or uncoated; in the secondary-

electron emission mode. Uncoated samples were also observed in the STEM mode in the FESEM as well. The TEM utilized was a Hitachi H-8000 analytical TEM operated at 200 kV and employing a goniometer-tilt stage. Bright and dark-field imaging was performed along with selected-area electron diffraction (SAED) analysis.

The morphology of the human epithelial (A549) cells following various exposure regimes with the nanoparticulate materials was also observed using light microscopy (Fisher Scientific Micromaster inverted microscope). Intervals of observation ranged from 48 h to 336 h; at 48 h intervals.

Results

Viability Assays

Figure 1 shows for comparison the Sytox (dead cell) results for the manufactured nanoparticulate materials including carbon surrogate nanoparticulate aggregates (BC, MWCNT-R, MWCNT-N) for short (48 h) and longer-term (336 h) exposure in culture.

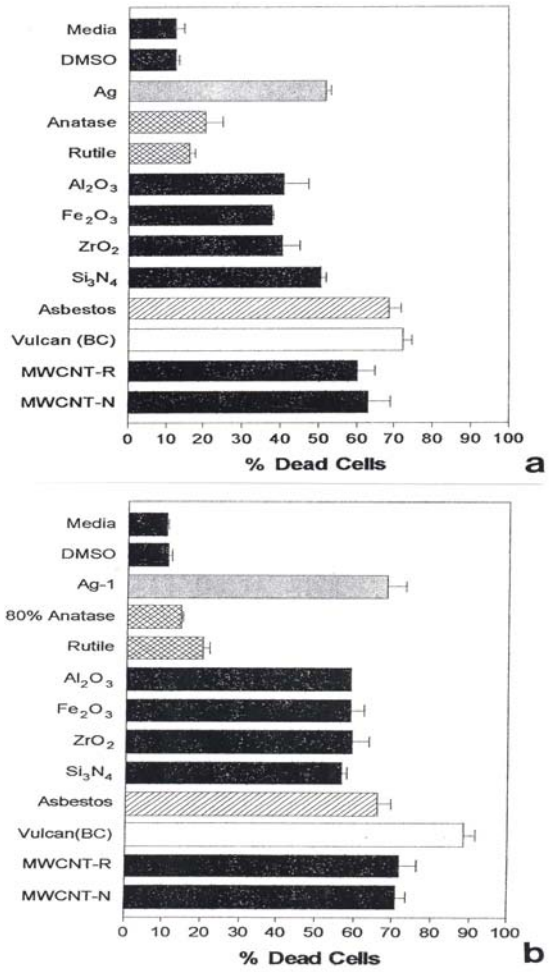

Figure 1: Cell death induced by manufactured nano-PM *in vitro* using human epithelial (A549) cells.

A549 cells were exposed to the indicated nano-PMs for 48 h (a) at 5 μg/mL or for 336 h (b) at 0.5 μg/mL. Media treated cells are the "untreated" control cells and DMSO-treated cells are the "vehicle-treated" control cells. Following the treatment period, cell death was determined by flow cytometry to determine the percentage of Sytox positive cells (dead cells). The data is presented as the mean ± SEM of triplicate samples and is one of three representative experiments.

In comparison, fig. 2 reproduces recent [41] direct filter contact cell (A549) viability results for the surrogate BC and MWCNT-R nanoparticulate materials and various carbonaceous (soot) nano-PM.

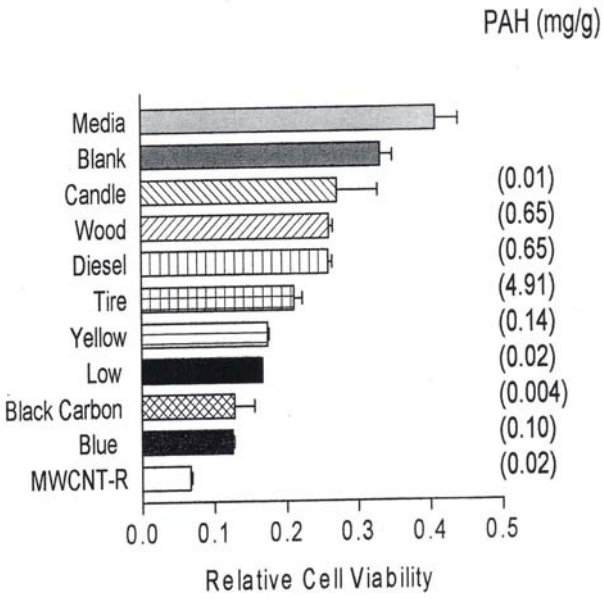

Figure 2: Relative cell viability assays for direct contact filter collections in 48 h cultures with human epithelial (A549) cells.

A549 cells were exposed to glass fiber filters on which the indicated materials were collected. Media-treated cells are the "untreated" control cells sands the blank are cells treated with a filter on which nothing had been collected. Following a 48 hrs exposure period, the filters were removed, the cells were harvested and assessed for relative cell viability by an MTT assays (as described elsewhere [42]). The data is presented as the mean ± SEM of triplicate samples and is one of two representative experiments.

Figure 2 also shows the corresponding, total PAH concentrations (in mg/g or thousand ppm) determined by Shi et al. [42]. It can be noted in Figs. 1 and 2 that all of the nanoparticulate materials exhibit some *in vitro* cytoxicity, and this increases with time. Moreover, the surrogate carbon nanoparticulate materials (BC, MWCNT-R and MWCNT-N) are the most cytotoxic, along with the blue-flame, natural gas soot nano-PM. The nano-silver PM is also highly cytotoxic along with the

chrysotile asbestos. As noted previously, Fig. 2 shows that there is no correlation between PAH content and A549 epithelial cell viability for soot nano-PM. While there is some increase in cytoxicity with longer exposure time (Fig. 1(b)), the general trends seem to be adequately represented by the 48 h assay shown in Fig. 1(a). It is interesting to note on comparing Fig. 1(a) and (b) that the chrysotile asbestos response is unchanged from 48 hrs to 336 hrs respectively. This is also true for the TiO_2 allotropes (rutile and anatase) which exhibit only slight cytotoxicity.

Figures 3-5 compare the A549 human epithelial cell morphologies and nanoparticle inclusions (endocytosed) as a function of exposure time for rutile (TiO_2), Fe_2O_3, and BC, respectively, while fig. 6 shows for comparison the corresponding results for the morphology of the A549 cells upon exposure to carbonaceous nano-PM on filters after 48 hrs. Cell death is generally indicated by cell rounding or reduction in cell density in contrast to the media with no nano-PM additions. These morphological variations and ingested nano-PM aggregates generally characterize the trends implicit on comparing Fig. 1(a) and (b) and Fig. 2.

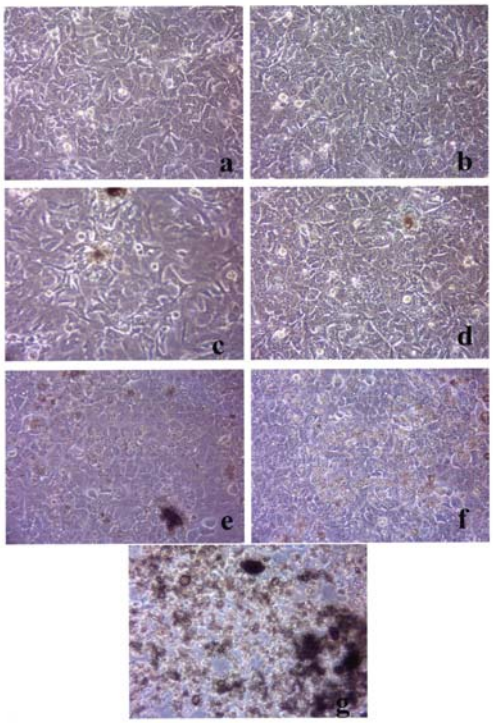

Figure 3: Light optical microscopy of A549 cell morphology suspended in TiO_2 (rutile).

A549 cells were cultured in the presence of 0.5 μg/mL of rutile for 48 hrs (a), 96 hrs (b), 144 hrs (c), 192 hrs (d), 240 hrs (e), 288 hrs (f) and 336 hrs (g) (the cells were given fresh media and rutile every 48 hrs). At each time point, the cells were photographed by light microscopy to assess overall morphology of the treated cells. Data was obtained at 40X magnification and is one of two representative experiments.

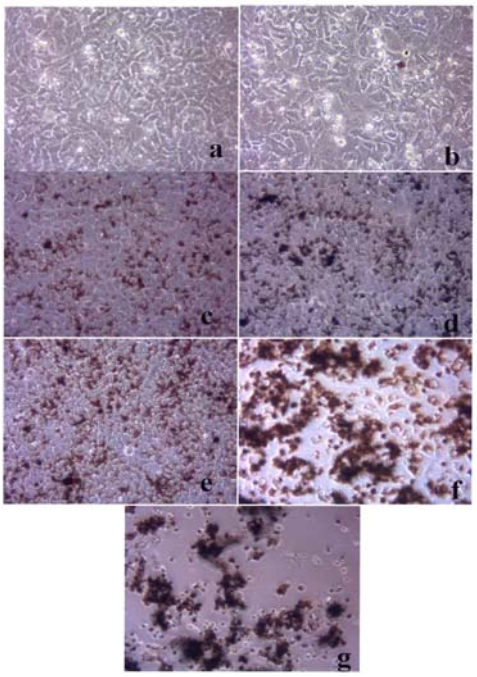

Figure 4: Light optical microscopy of A549 cell morphology suspended in Fe_2O_3.

A549 cells were cultured in the presence of 0.5 μg/mL of Fe_2O_3 for 48 hrs (a), 96 hrs (b), 144 hrs (c), 192 hrs (d), 240 hrs (e), 288 hrs (f) and 336 hrs (g) (the cells were given fresh media and rutile every 48 hrs). At each time point, the cells were photographed by light microscopy to assess overall morphology of the treated cells. Data was obtained at 40X magnification and is one of two representative experiments.

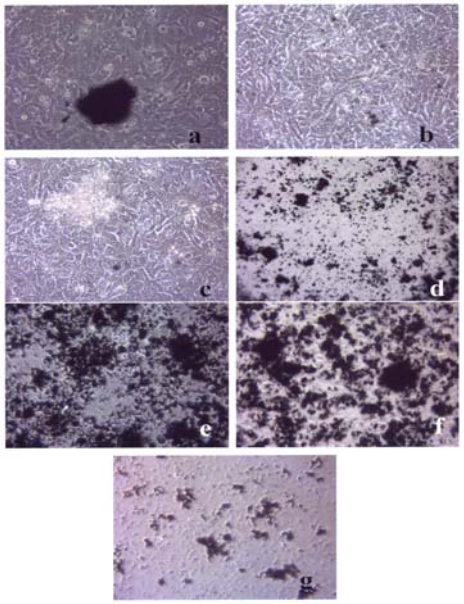

Figure 5: Light optical microscopy of A549 cell morphology treated with black carbon.

A549 cells were cultured in the presence of 0.5 μg/mL of black carbon for 48 hrs (a), 96 hrs (b), 144 hrs (c), 192 hrs (d), 240 hrs (e), 288 hrs (f) and 336 hrs (g) (the cells were given fresh media and rutile every 48 hrs). At each time point, the cells were photographed by light microscopy to assess overall morphology of the treated cells. Data was obtained at 40 X magnification and is one of two representative experiments.

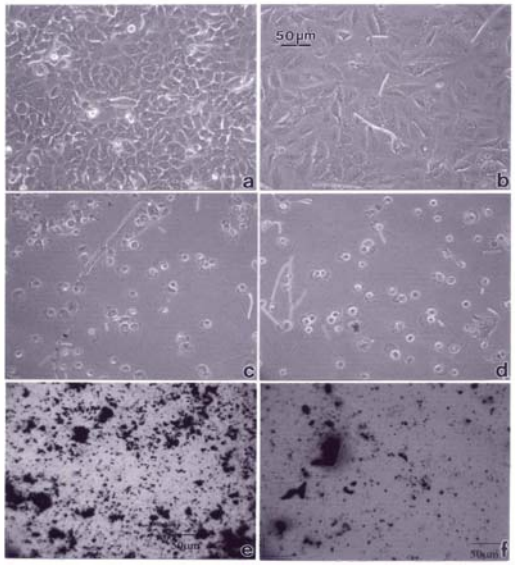

Figure 6: Comparative light optical microscopy (A549) cells after direct filter contact assays.

A549 cells were photographed at 40X after 48 h exposure to media only (control) (a), a blank filter (b), a blue flame natural gas soot filter (c), a yellow flame natural gas soot filter (d), a commercial BC on filter (e), and a MWCNT-R aggregate on filter (f). Data is one of two representative experiments.

Cytokine Response

Notable IL-6 release was observed for Ag, Fe_2O_3, ZrO_2, chrysotile asbestos, and the carbon nano-PM surrogates (BC, MWCNT-R, and MWCNT-N) as illustrated in Fig. 7(a) while notable IL-8 release was observed for the Ag, Fe_2O_3, chrysotile asbestos, and the carbon surrogate nano-PM as shown for comparison in Fig. 7(b). The IL-6 release relative to the media and DMSO control cultures (for the human epithelial (A549) cells) ranged from roughly 3X for nano-Ag, to >6X for the MWCNT-N nanoparticulate material (Fig. 7(a)). In contrast, the IL-8 release relative to the media and DMSO control cultures ranged from <2X for the nano-Ag to ~1.5X for the MWCNT-N nanoparticulate material. Of course these comparisons are within the respective ranges of relative measurements in Figs. 7(a) and (b), respectively and do not represent actual differences in concentration data. This difference in the relative IL-6 release in contrast to the IL-8 release for the carbon nanoparticulate materials (BC, MWCNT-R, MWCNT-N) is consistent with cytokine release (or secretion) data for carbon and carbonaceous PM composing mineral dusts along roadsides determined from human bronchial epithelial cell (BEAS-2B) culture assays recently reported by Veranth, et al. [46]. There was no detectable IL-6 or IL-8 release for the carbonaceous PM on filters.

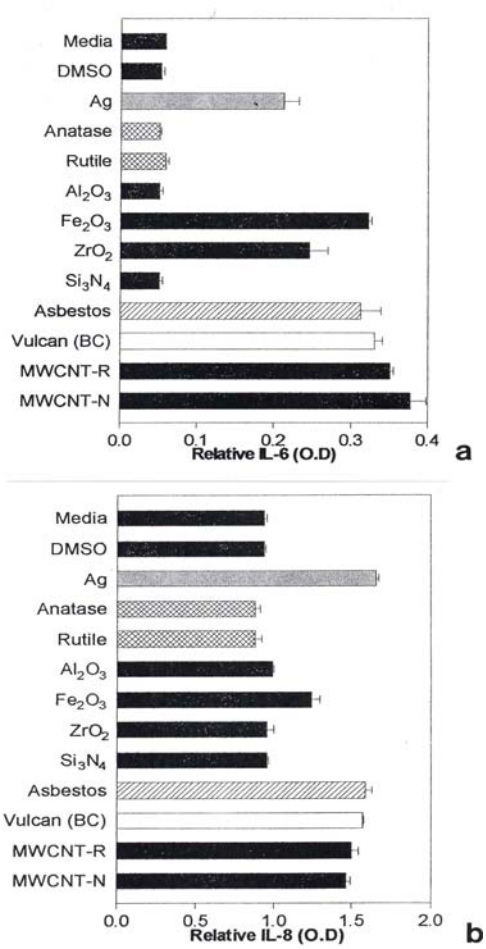

Figure 7: Production of cytokines by A549 cells upon exposure to nano-PMs.

A549 cells were exposed to 5 μg/mL of the indicated nano-PMs for 48 h and supernatants were assessed for the production of IL-6 (a) or IL-8 (b). Media-treated cells are the "untreated" control cells and DMSO-treated cells are the "vehicle-treated" control cells. Following the treatment period, a sandwich ELISA was conducted to evaluate the presence of cytokine in the cell supernatants. The data is presented as the mean ± SEM of duplicate wells and is one of two representative experiments.

ROS Analysis

Figure 8 is representative of the ROS generated by the A549 cells upon treatment with the manufactured

nanoparticulate materials as well as the carbon and carbonaceous (soot) nano-PM in reference to hydrogen peroxide (H_2O_2) and the media or DMSO controls. The generation of ROS fell into four general categories: I) no production of ROS in comparison to controls (TiO_2 – rutile); II) an intermediate level of ROS production which was either equal to or slightly above that generated by the H_2O_2 positive control (Al_2O_3, TiO_2 – anatase, and SiN_3); III) high levels of ROS production, above that generated by the positive control (Ag, Fe_2O_3, ZrO_2, asbestos and MWCNT-R); and IV) extremely high levels of ROS that are produced very rapidly (black carbon and MWCNT-N).

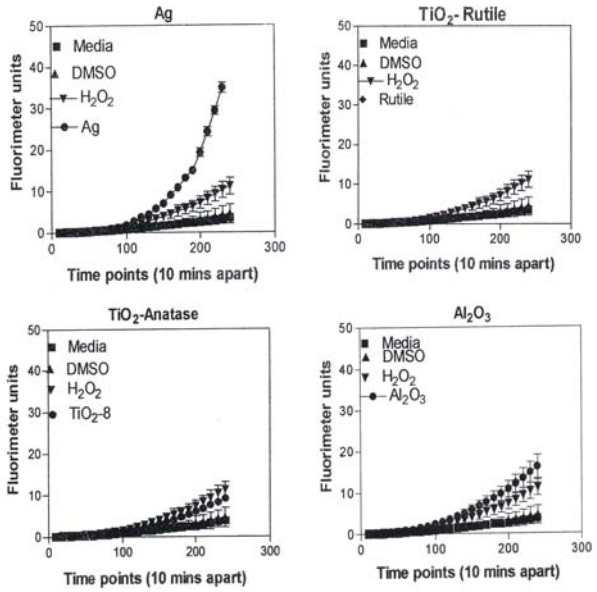

Figure 8: ROS generation by A549 cells upon treatment with manufactured nano-PM.

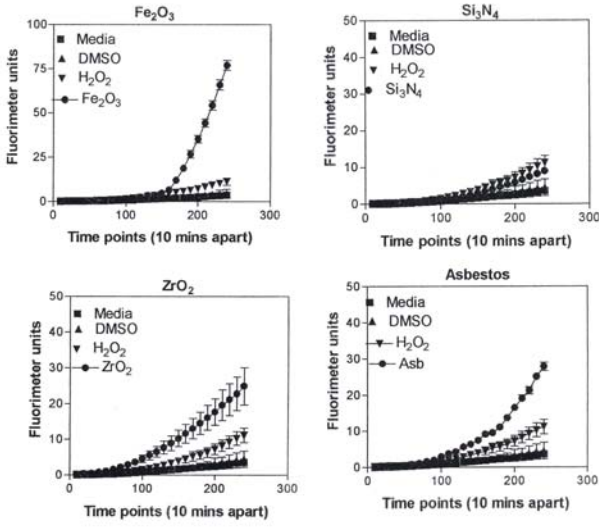

Figure 9: ROS generation by A549 cells upon treatment with manufactured nano-PM.

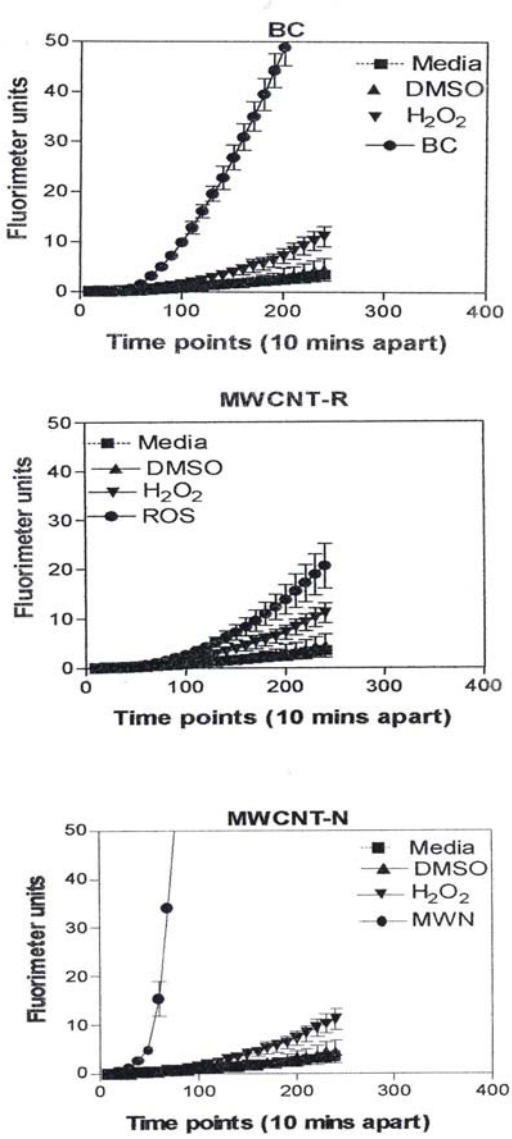

Figure 10: ROS generation by A549 cells upon treatment with manufactured nano-PM.

A549 cells were exposed to 5 μg/mL of nano-PMs for 48 h; the cells were then washed and assessed for the production of ROS using dye that becomes fluorescent in an oxidative environment. Media-treated cells and H_2O_2-treated cells were used as negative and positive controls, respectively and DMSO-treated cells functioned as a vehicle control. Presence of ROS was determined by the relative increase in fluorescence over time. The nano-PMs generated no detectable levels of ROS (represented by rutile in Fig. 8, intermediate levels of ROS (equal to that generated by the positive control as represented by Al_2O_3 in Fig. 8), high levels of ROS (as represented by Ag in Fig. 8), and extremely high levels of ROS (as represented by black carbon in Fig. 10). The data is presented as the mean ± SEM of quadruplicate wells and is one of three representative experiments.

In Figure 9, the levels of ROS produced in response to carbon and carbonaceous (soot) nano-PM is shown. The materials were obtained from mass collections of combustion soot or mass collection of natural gas kitchen burner soot on glass fiber filters. All of these materials generated ROS although to different extents; above background but not equal to the H_2O_2 control (candle, diesel, and wood) or equal to the H_2O_2 control (tire, yellow flame, blue flame, and low flame soots). The ROS data is somewhat consistent with the IL-6 cytokine data (Fig. 7) in that the materials that generated ROS above the levels induced by H_2O_2 (Fig. 10) also induced the production/secretion of IL-6.

Microstructures and Nanostructural Issues

Observations and comparisons of the morphologies of aggregated nanoparticles, including their crystallinity, chemical compositions and nanostructures (including intercalation of irregular graphene fragments and PAH isomers composing primary soot nanoparticles, as well as specific surface area) and related phenomena have not revealed any significant or obvious toxicitiy-related microstructural mechanisms [12, 15, 17, 39-42, 47]. However, there are clearly notable trends (Figs. 1, 2, 7, 13) with cytotoxic cellular response, cytokine release, and ROS production for several of the nano-PM examined in this study. These include the silver, Fe_2O_3, BC, MWCNT-R, and especially the MWCNT-N nano-PM. Of the carbonaceous nano-PM, the kitchen burner (natural gas) combustion PM exhibits a notable response.

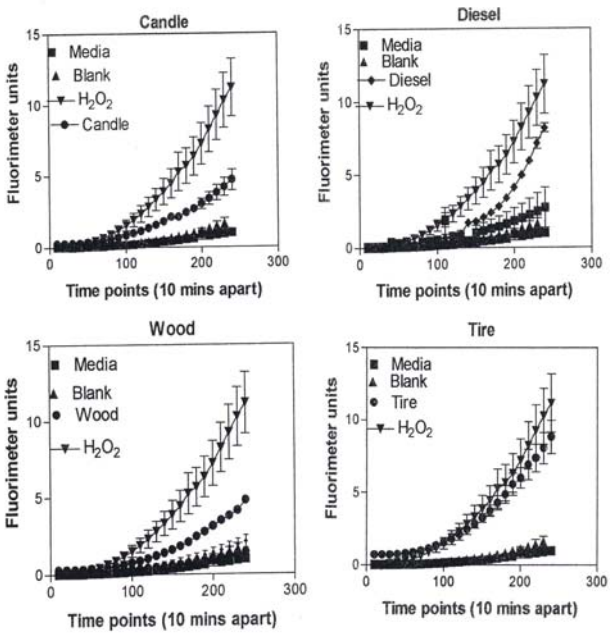

Figure 11: ROS generation by A549 cells upon treatment with mass collections of combustion soot nano-PM on glass fiber filters.

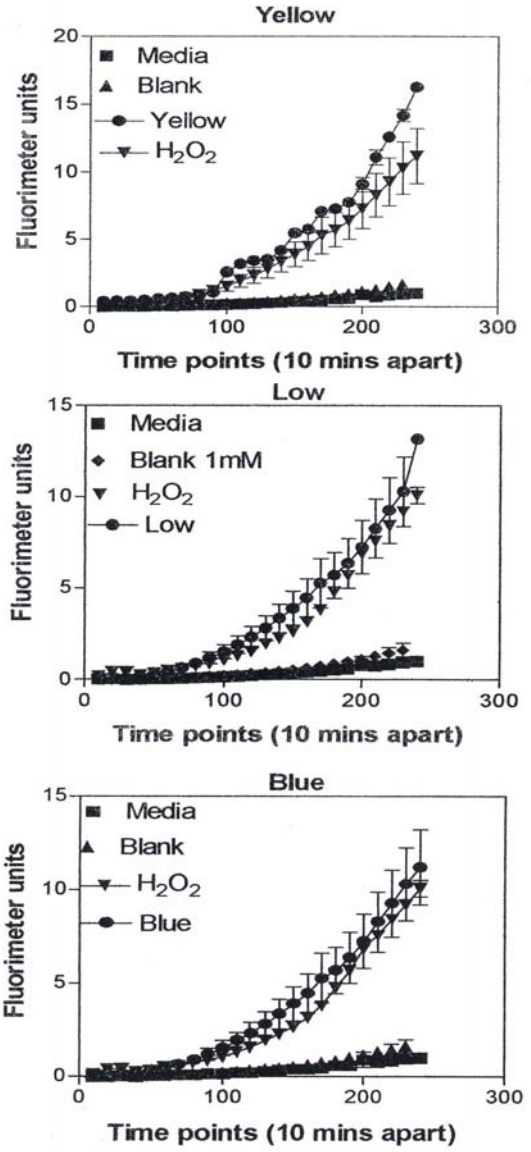

Figure 12: ROS generation by A549 cells upon treatment with mass collections of combustion soot nano-PM on glass fiber filters.

A549 cells were exposed to 5 μg/mL of nano-PMs for 48 h; the cells were then washed and assessed for the production of ROS using dye that becomes fluorescent in an oxidative environment. Media-treated cells and H_2O_2-treated cells were used as negative and positive controls, respectively and DMSO-treated cells functioned as a vehicle control. Presence of ROS was determined by the relative increase in fluorescence over time. The nano-PMs generated low levels of ROS levels that were above background but below the positive controls (represented by candle soot in (a)) and intermediate levels of ROS equal to that of the positive control (represented by tire soot in (b)). The data is presented as the mean ± SEM of quadruplicate wells and is one of three representative experiments.

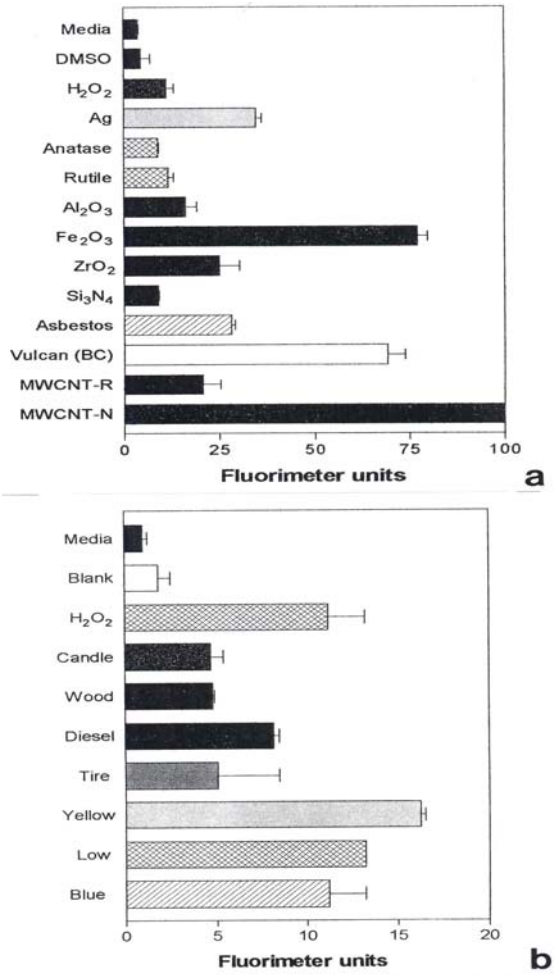

Figure 13: Summary of ROS generation.

ROS generation by A549 cells 240 minutes after the addition of the DCA-DF dye following a 48 hrs treatment with manufactured nano-PM (b) or combustion soot nano-PM (b). The data is presented as the mean ± SEM of quadruplicate wells and is one of three representative experiments.

Figure 14 compares the Ag and Fe_2O_3, TEM images and SAED patterns. Both are cubic crystal structures and the primary particle morphologies and size distributions are very similar. Unlike Ag, which has a wide range of systemic hazards for humans versus animals and notable antibacterial effects on humans [48], Fe_2O_3, is generally less hazardous with no corresponding antibacterial features. But transition metal ions such as Fe, Ni, Ti, etc. have long been tauted as important mediators in cytokine release [6] and ROS production n[6,31]. In contrast to fig. 14, fig. 15 shows a considerable morphological difference between the arc-evaporation produced MWCNT-R nano-PM, and the Ni-nanoparticle catalyzed production of MWCNT-N. The only significant microstructural or nanostructural difference here may be the Ni catalyst particles which, as discussed by others, may symbiotically exaggerate the cytokine (IL-6) release and ROS production.

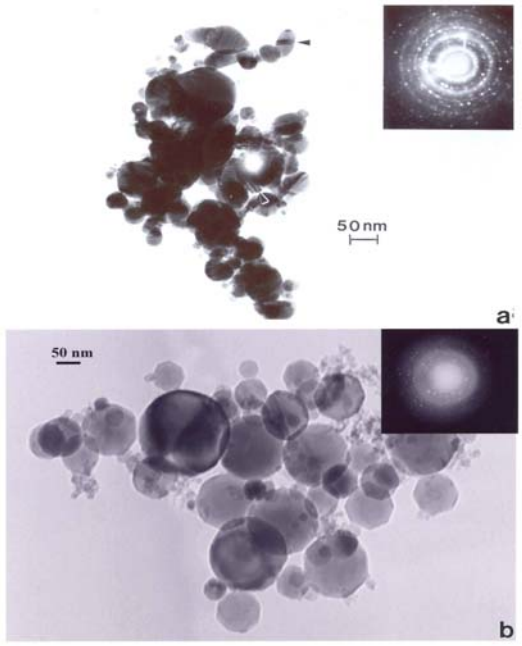

Figure 14: TEM bright-field images of manufactured nano-PM. (a) Silver, (b) Fe_2O_2. SAED pattern inserts illustrate cubic crystal structures. (From Soto, et al. [48]).

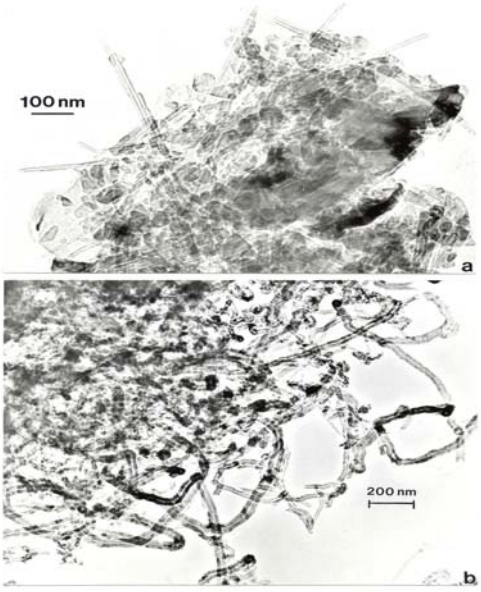

Figure 15: TEM images of commercial multiwall carbon nanotube aggregate materials. (a) MWCNT-R, arc-evaporation growth aggregate PM, (b) MWCNT-N, Ni nano-catalyst grown aggregate PM.

Figure 16 compares the commercial BC and the diesel PM aggregates which do not exhibit any notable morphological or primary spherule particle variations. As shown in fig. 2, the significantly higher PAH content of the diesel PM might suggest a more cytotoxic-related

nanoparticulate material [49-51], but the DPM produces no cytokine and a factor of 6 less ROS (Fig. 13).

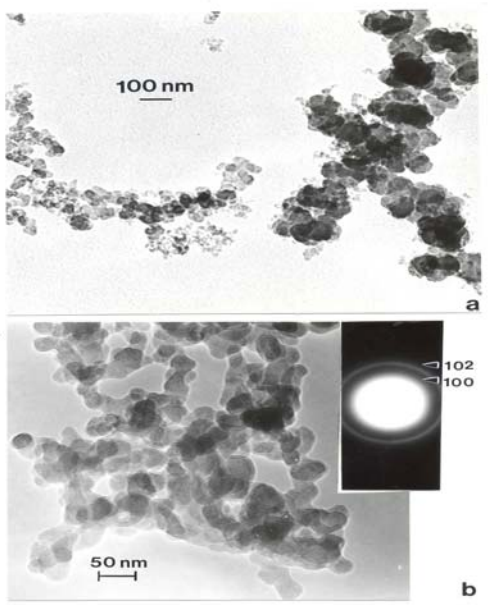

Figure 16: TEM images of commercial (Cabot Corp.) BC (a) and diesel particulate matter (DPM) from a heavy-duty truck exhaust collected by thermal precipitation (b). The SAED pattern insert in (b) shows prominent graphite reflections. (From Murr, et al. [17]).

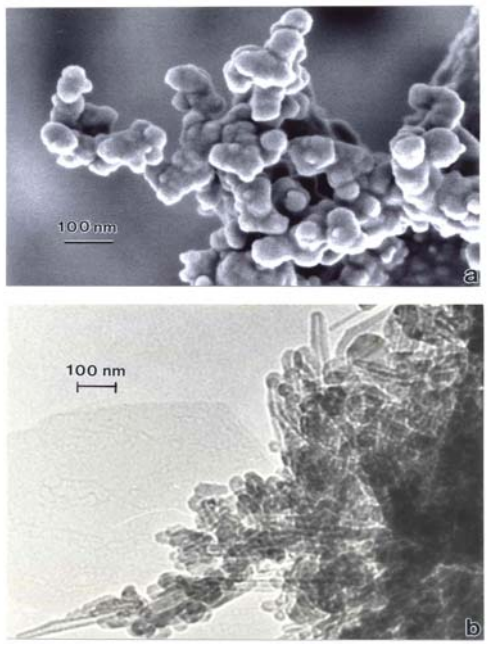

Figure 17: (a) FESEM image of yellow flame natural gas kitchen burner soot collected on glass fiber filter. (b) TEM bright-field image of MWCNT aggregate PM collected by thermal precipitation above a natural gas kitchen burner blue flame.

Correspondingly, fig. 17 compares the natural gas flame (yellow) soot and efficient low blue/regular blue flame emission of MWCNT aggregate/soot PM mixture. While Fig. 17(a) and (b) exhibit a marked microstructural/nanostructural difference, comparison of Fig. 17(a) with the DPM in Fig. 16(b) or the BC in Fig. 16(a) does not provide any compelling evidence for the marked differences in cytotoxic-related responses shown on comparing Figs. 1, 2, and 13. It is particularly significant to note that the BC in Fig. 16(a) and the natural gas yellow flame soot nano-PM appear to be nearly identical in microstructure/nanostructure, and the PAH content is also very similar (Fig. 2), and correspondingly much lower than the DPM shown in Fig. 16(b). It might be recalled that in the recent work of Jung, et al. [35], flame-derived soot nano-PM induced ten times the ROS response in surrogate lung fluid than BC. This significant variance is not supported in the ROS data shown on comparing Fig. 13(a) and (b) where collectively the BC an MWCNT surrogate PM is more than a factor of 2 greater ROS producer than the collective natural gas (kitchen burner) flame nano-PM.

Discussion

Salvi and Holgate [5], among others, have proposed that nano-PM toxicity and cytotoxicity ultimately involve some form of mediated generation of ROS. In the human body nano-PM penetrates the interstitium and contacts interstitial macrophages which release ROS that enter the blood stream and lead to cardiovascular dysfunction, e.g., COPD. ROS generation has also been associated with asbestos carcinogenicity as well as high molecular weight PAHs [31, 32, 49]. While soots with absorbed PAHs, and PAHs alone, such as benzo[a]pyrene are able to produce ROS [50], recent work by Gerde, et al. [51] have concluded that inhalation exposure to DPM with adsorbed PAHs is likely dominated by the desorbed PAH fraction deposited on the lining layer of the conducting airway, and it is unknown whether the range of toxicity and related respiratory health effects of DPM are a consequence of the PAHs or the intrinsic turbostratic graphene structure of primary nano-spherules composing DPM [3,31,52]. Nikula et al. [53] also concluded that the organic fraction (presumably intercalated PAHs) of DPM may not play an important role in its carcinogenicity in rats, while Heinrich, et al. [54] and Brightwell et al. [55] demonstrated that a pulmonary carcinogenic response in rates required the presence of DPM and not diesel exhaust gases. Heinrich et al. [56] also demonstrated that the so-called carbon core of DPM was mainly responsible for the occurrence of diesel engine exhaust-related lung tumors in rats. This suppressed role of PAHs in ROS production *in vivo* is supported by the ROS release data shown summarized in this study in Fig. 13; as this relates to the total PAH content of nano (soot) – PM shown in Fig. 2.

Amongst the carbon and carbonaceous nanoparticulate materials in this study, DPM did not exhibit either extensive cytotoxicity (A549 human epithelial cell death or viability decline (Fig. 2)) or ROS production (Fig. 13(b)) in contrast to natural gas flame nano-PM (soot) components, BC, or MWCNT aggregate PM; especially the MWCNT-N catalytically grown aggregate PM. Neither did the other carbonaceous nano-PM (candle, wood, or tire PM). The cell death, cytokine release, and ROS production associated with the BC and Fe_2O_3, were particularly significant. Transition metal components of ultrafine PM have been hypothesized to be important factors in toxicity [57,58], and transition metals (Ni, Ti, Fe, Cu especially) have been associated with carcinogenicity and hypoxia [59]. However, the cytotoxic response of the TiO_2 in this study was insignificant in contrast to many *in vivo* and *in vitro* studies where TiO_2 nano-PM in particular has been shown to induce oxidative injury, inflammation, cytotoxicity, and the like [33,60-62].

At the risk of introducing some speculation, it may be useful to explore the context in which the results of this study may be important. First, there is the evidence that many carbonaceous nano (soot)-PM especially prominent in the outdoor air: diesel, wood, or tire may not, under more normal (or low) concentrations pose more concern for respiratory health than indoor air with varieties of natural gas combustion soots, especially in kitchens. Tire wear, especially BC release, may contribute significantly to respirable, inflammatory nano-PM, while natural hematite (Fe_2O_3,) may, as nano-PM, pose additional inflammatory concerns in some areas; especially in the context of inducing synergistic effecdts in concert with BC or other carbonaceous nanoparticulate materials.

Of particular concern may be the significant, short-term production of ROS by BC, Fe_2O_3, natural gas-derived carbonaceous (soot) nano-PM, and multiwall carbon nanotubes which often compose natural gas combustion PM, and of course are finding their way into a range of commercial products and applications as nanotechnology, as it applies to commercial product development. Little is known about dose-related issues and even less is known about intermittent-long term exposures which are characteristic of natural gas or even other gas cooking on a regular basis. Microenvironments which contain higher concentrations of mineral dusts which include wear-related BC (near major highways) or regions compromised by various burning cycles (wood, tire, or agricultural burning) may also be associated with higher incidences of compromised health issues such as asthma. At the very least, the results of this study should encourage epidemiological strategies consistent with these prospects.

Summary and Conclusions

- Cytotoxicity assays utilizing an immortalized human epithelial cell line (A549) indicated significant cell death for exposure to a range of manufactured nanoparticulate materials: Ag, Al_2O_3, Fe_2O_3, ZrO_2, Si_3N_4, chrysotile asbestos, BC, and two types of MWCNT aggregate PM; after 2 days and 2 weeks exposure respectively, *in vitro*.
- Decreasing cell viability (increasing cell death) was observed in the following order for filter-collected carbonaceous nanoparticulate (soot) PM, and surrogate MWCNT-R aggregate PM after 48 H (2 days) in contact with the human epithelial cells (A549) in culture: candle PM< wood PM< diesel PM< tire PM< yellow flame natural gas (fuel rich) PM, low flow, blue-flame natural gas PM< MWCNT-R aggregate PM. The implications are that nano-PM released from kitchen natural gas burners is more cytotoxic than other carbonaceous (soot) nano-PM; including other cooking-related kitchen soot.
- Cytokine release (IL-6) was detected for the Ag, Fe_2O_3, ZrO_2, chrysotile asbestos, BC, and the MWCNT aggregate PM in the human epithelial cell line (A549).
- Cytokine release (IL-8) was detected for the Ag, Fe_2O_3, chrysotile asbestos, BC, and the two types of MWCNT aggregate PM in the human epithelial cell line (A549).
- The cytotoxic response for carbonanceous (soot) nano-PM was not correlated with total PAH content. The lowest PAH content was associated with the kitchen natural gas burner nano-PM emissions and the MWCNT-R aggregate PM, which exhibited the greatest propensity for cell (A549) death.
- Significant reactive oxygen species (ROS) production was detected in *in vitro* assays for the Ag, Fe_2O_3, ZrO_2, chrysotile asbestos, BC, and the MWCNT aggregate PM, especially the MWCNT-N PM commercially produced utilizing Ni nano-PM catalysts.
- ROS was detected at or slightly above the reference H_2O_2 level only for the kitchen natural gas burner nano-PM emissions: yellow flame, low-flow blue flame, and high-flow (normal) blue flame operation although the other carbonaceous (soot) PM exhibited ROS slightly above the media and blank filter control.
- Very significant cytotoxic responses (cell death, proinflammatory cytokine release, and ROS production for an immortalized human epithelial cell line (A549) was observed for Fe_2O_3, nano-PM, BC, MWCNT aggregate PM, and kitchen natural gas burner nano-PM emissions, all of which are components of ambient environments and particularly microenvironments to which humans may be intermittently exposed over long time periods. These responses may be related to both short-term and long-term health effects in humans.
- There is no clear mechanism either for provoking cytotoxic responses or for related respiratory, inflammatory responses in humans. Parameters such as PM size, morphology, crystallinity, chemistry, specific surface area, or related phenomena have not

been identified as significant contributors to cytotoxic responses.

Acknowledgments: We are pleased to acknowledge the following support: a University of Texas System Louis Stokes Alliance for Minority Participation (LSAMP) Bridges to Doctorate Fellowship (KFS); The University of Texas Alliance for Graduate Education and the Professoriate (AGEP) Program (KFS); an EPA Student Scholarship (KFS); NIH Research Centers at Minority Institution (RCMI) Grant (G12RR08124) (KMG); Southwest Consortium for Environmental Research and Policy (SCERP), Projects A-04-1 and A-05-1 (KMG and LEM); a Mr. and Mrs. MacIntosh Murchison Endowment at the University of Texas at El Paso (LEM); Grant No. 1S11ES01339-01A1 from the U.S. National Institute of Environmental Health Sciences (NIEHS) – NIH. The contents of this paper are solely the responsibility of the authors and do not necessarily represent the official views of SCERP, NIEHS, NIH or any other supporting agency. We also acknowledge the careful reading of the manuscript by Dr. Scott Burchiel, UNM HSC College of Pharmacy, and for his comments.

References

1. Samet, J. M.; Doninici, F.; Curriero, F. C.; Coursad, I.; Zeger, S. C.: Fine particulate air pollution and mortality in 20 U.S. cities, 1987-1994. N. *Engl. J. of Med.* **2000**, *343(24)*, 1742-1749.
2. Ziqiang, Q.; Siegmann, K.; Keller, A.; Matter, U..; Scherrer, L.; Siegmann, H. C.: Nanoparticle air pollution in major cities and its origin. *Atmos. Environ.* **2000**, *34*, 443-451.
3. Oberdörster, G.: Pulmonary effects of inhaled ultrafine particles. *Int. Arch. Occup. Environ. Health*, **2001**, *74*, 1-8.
4. Lighty, J. S.; Veranth, J. M.; Sarofim, A. F.: Combustion aerosols: factors governing their size and composition and implications to human health. *J. Air & Waste Manage. Assoc.*, **2000**, *50*, 1565-1618.
5. Salve, S.; Holgate, S. T.: Mechanisms of particulate matter toxicity, *Clinical and Exp. Allergy*, **1999**, *29*, 1187-1194.
6. Donaldson, K..; Stone, V.; Clouter, A.; Renwick, L.; MacNee, W.: Ultrafine particles, *Occup. Environ. Med.* **2001**, *58*, 211-216.
7. Frampton, M.W.; Systemic and cardiovascular effects of airway injury and inflammation: Ultrafine particle exposure in humans. *Environ. Health Perspectives*, **2001**, *109 (Suppl. 40)*, 529-532.
8. Chalupa, D.C.; Morrow, P. E.; Obesdörster, G.; Utell, M. J.; Frampton, M.W.; Ultrafine particle deposition in subjects with asthma, *Environ. Health Perspectives*, **2004**, *112 (8)*, 879-882.
9. Jansen, K. L.; Larson, T. V.; Koenig, J. O.; Mar, T. F.; Fields, C.; Stewart, J.; Lippmann, M.: Associations between health effects and particulate matter and black carbon in subjects with respiratory disease. *Environ. Health Perspectives*, **2005**, *113(12)*, 1741-1746.
10. deHaar, C.; Hassing, I.; Bol, M.; Bleumink, R.; Pieters, R.: Ultrafine but not fine particulate matter causes airway inflammation and allergic airway sensitization to co-administered antigen in mice. *Clin. And Exper. Allergy*, **2006**, *36*, 1469-1479.
11. Renwick, L. C.; Brown, D.; Clouter, A.; Donaldson, K.: Increased inflammation and altered macrophage chemotactic response caused by two ultrafine particle types. *Occup. Environ. Med.,*. **2004**, *61*, 442-447.
12. Soto, K. F.; Carrasco, A.; Powell, T. G.; Murr, L. E.; Garza, K. M.: Biological effects of nanoparticulate materials. *Mater. Sci. Engng.*, **2006**, 26, 1421-1427.
13. Pope, C. A. III; Dockery, D. W.: Health effects of fine particulate air pollution: lines that connect. *J. Air & Waste Manage. Assoc.* **2006**, 56, 709-742.
14. Nikasinovic, L.; Just, J.; Sahraousi, F.; Jeta, N.; Grimfeld, A; Mamas, I.: Nasal inflammation and personal exposure to fine particles PM 2.5 in asthmatic children. *J. Allergy Clin. Immunol.*, **2006**, *117 (6)*, 1382-1387.
15. Murr, L. E.; Soto, K. F.; Garza, K. M.; Guerrero, P. A.; Martinez, F.; Esquivel, E.V.; Ramirez, D. A.; Shi, Y.; Bang, J. J; Venzor III, J.: Combustion-generated nanoparticulates in the El Paso, TX/USA/Juarez, Mexico metroplex: Their comparative characterization and potential for adverse health effects. *Int. J. Environ. Res. Public Health*, **2006**, *3(1)*, 48-66.
16. Lam, C-W.; James, J. T.; McCluskey, R.; Arepalli, S.; Hunter, R. C.: A review of carbon nanotube toxicity and assessment of potential occupational and environmental health risks. *Crit. Rev. Toxicol.* **2006**, *36*, 189-217.
17. Murr, L. E.; Soto, K. F.; Garza, K. M.: Health hazards of manufactured, natural, environmental and other anthropogenic atmospheric nanoparticulate materials: past, present and future, Chap. 1 in "Biomaterials and biomedical Engineering", *A. Oechsner, W. Ahmed and N. Ali (eds.), Trans Tech. Publishers, Switzerland*, **2008**.
18. Kelly, J.: Cytokines of the lung. *Amer. Rev. Respir. Disease*, **1990**, *141*, 765-788.
19. Dricsoll, K. E.: Cytokines and regulation of pulmonary inflammation, In: "Toxicology of the Lung", D. E. Gardner, J. D. Crapo, R. D. McClellan (eds.), Taylol & Francis, Ann Arbor, **1999**, 149-172.
20. Theze, J.: "the Cytokine Network and Immune Functions", *Oxford Univ. Press, New York*. **1999**.
21. Hetland, R. B.; Refsnes, M.; Myran, T.; Johansen, B.V.; Uthus, N.; Schwarts, P. E.: Mineral and/or metal content and critical determinants of particle-induced release of IL-6 and IL-8 from A549 cells, *J. Toxicol. Environ. Health*, **2000**, *A60*, 47-65.

22. Hetland, R. B.; Casser, F. R.; Refsnes, M.; Schwarze, P. E.; Lag, M.; Boere, A. F. G.; et al.: Release of inflammatory cytokines, cell toxicity and apoptosis in epithelial lung cells after exposure to ambient air particles of different size fractions. *Toxicol. In Vitor*, **2004**, *18*, 203-212.
23. Becker, S.; Soukup, J. M.; Sioutas, C.; Cassee, F. R.: Response of human alveolar macrophages to ultrafine, fine, and coarse urban air pollution particles, *Exper. Lung Res.* **2003**, *29*, 29-44.
24. Veronesi, B.; deHaar, C.; Lee, L.; Oortgiesen, M.: The surface charge of visible particulate matter predicts biological activation in human bronchial epithelial cells, *Toxicol. Appl. Pharmacol.*, **2002**, *178*, 144-154.
25. Koyoma, Si; Sato, E.; Nomura, H.; Kubo, K.; Miura, M.; Yamashita, T.; et al.: The potential of various lipopolylsaccharides to release IL-8 and G-CSF, *Amer. J. Physcol. Lung Cell Mol. Physiol.*, **2000**, *278*, L658-L666.
26. Nelson, Si; Martin, T. R.: "Cytokines in Pulmonary Disease: Infection and Inflammation Lung Biology in Health and Disease". *Marcel Dekker, Inc., New York*. **2000**, *vol. 1411*.
27. van Eeden, S. F.; Tan, W. C.; Suwa, T.; Fujii, T.; et al.: Cytokines involved in systemic inflammatory response induced by exposure to particulate matter air pollutants (PM10), *Amer. J. Respir. Crit. Care Med.*, **2001**, *164*, 826-830.
28. Chung, K. F.: Cytokines in chronic obstructive pulmonary disease, *Environ. Respir. J.*, **2001**, *18*, 505-595.
29. Jacobson, M.: Reactive oxygen species and programmed cell death, *Trends in Biochem.* **1996**, *21*, 83-86.
30. Li, N.; Sioutas, C.; Cho, A.; Schmitz, D.; Misra, C.; Sempf, J.; CNAG, M.; Oberley, T.; Froines, J.; Nel, A.: Ultrafine particulate pollutants induce oxidative stress and mitochondrial damage, *Environ. Health Perspecitves*, **2004**, *111*, 455-460.
31. Manning, C. B.; Vallyathan, V.; Mossman, B. T.: Diseases caused by asbestos: mechanisms of injury and disease development, *Int. Immunopharmacol.* **2002**, *2*, 191-200.
32. Shukla, A.; Ramos-Nino, M.; Mossman, B. T.; Cell signaling and transcription factor activation by asbestos in lung injury and disease, *Int. J. Biochem. & Cell Biol*. **2003**, *35*, 1198-1209.
33. Nel, A.; Xia, T.; Mädler, L.; Li, N.: Toxic potential of materials at the nanolevel, *Science*, **2006**, 311, 622-627.
34. Imlay, J. A.; Linnk S.: DNA damage and oxygen radical toxicity, *Science*, **1988**, *240*, 13032-1309.
35. Jung, H.; Guo, B.; Anastasio, C.; Kennedy, I.M.: Quantitative measurements of the generation of hydroxyl radicals by soot particles in a surrogate lung fluid, *Atmos. Environ.* **2006**.
36. Halliwell, B.; Gutteridge, J. M. C.: "Free Radicals in Biology and Medicine", *Oxford Univ. Press, Oxford*, **1999**.
37. Polansky, H.: "Microcompetition with Foreign DNA and the Origin of Chronic Disease, *CBCD Publishing, Rochester, N.Y.* **2003**.
38. Murr, L. E., "Electron and Ion Miroscopy and Microanalysis: Principles and Applications, *Marcel Dekker, Inc., N.Y.*, **1991**.
39. Soto, K. F.; Carrasco, A.; Powell, T. G.; Garza, K. M.; Murr, L. E.: Comparative in vitro cytotoxicity assessment of some manufactured nanoparticulate materials characterized by transmission electron microscopy, *J. Nanoparticle Res.*, **2005**, *7*, 145-169.
40. Soto, K. F.; Garza, K. M.; Murr, L. E.; Cytotoxic effects of aggregated nanomaterials, *Acta Biomaterialia*, **2007**, *3*, 357-358.
41. Soto, K. F.; Garza, K. M.; Murr, L. E.: Direct contact cytotoxicity assays for filter-collected carbonaceous (soot) nanoparticulate material and observations of lung cell response, *Atmospheric Environment*, **2008**, *42*, 1970-1982.
42. Shi, Y.; Murr, L. E.; Soto, K. F.; Guerrero, P. A.; Lee, W-Y.; Ramirez, D. A.: Characterization and comparison of speciated atmospheric carbonaceous (soot) particulates and their polycyclic aromatic hydrocarbon contents in the context of the Paso del Norte airshed along the U.S.-Mexico border, *Polycyclic Aromatic Compounds*, **2007**, *27*, 361-400.
43. Murr, L. E.; Bang, J. J.; Esquivel, E. A.; Guerrero, P.A.; Lopez, D. A.: Carbon nanotubes, nanocrystal forms, and complex nanoparticle aggregates in common fuel gas combustion streans, *J. Nanoparticle Res.*, **2004,** *6*, 241-251.
44. Bang, J. J.; Trillo, E. A.; Murr, L. E.: Utilization of selected area electron diffraction patterns for characterization of air submicron particulate matter collected by a thermal precipitator, *J. Air & Waste Manag. Assoc.* **2003**, *53*, 227-236.
45. Murr, L. E., Bang, J. J.: Electron microscopy comparisons of fine and ultrafine carbonaceous and nano-carbonaceous, airborne particulates, *Atmos. Environ.* **2003**, *37*, 4795-4806.
46. Veranth, J. M.; Moss, T. A.; Chow, J. C.; Labban, R.; Nichols, W. K.; Walton, J. C.; Watson, J. G.; Yost, G.S.: Correlation of *in vitro* cytokine responses with the chemical composition of soil-derived particulate matter, *Environ. Health Perspective*, **2006**, *114 (3)*, 341-349.
47. Warheit, D. B.; Webb, T. R.; Sayes, C. M.; Calvin, V. L.; Reed, K. C.: Pulmonary instillation studies with nanoscale TiO_2 rods and dots in rats: Toxicity is not dependent upon particle size and surface area, *Toxicol Sci.* **2006**, *91 (1)*, 227-236.
48. Soto, K. F.; Carrasco, A.; Powell, T. G.; Murr, L. E.; Garza, K. M.: Biological effects of nanoparticulate materials, *Mater. Sci. Engng.* **2006**, *C26*, 1421-1427.

49. Herndon, W. C.: quantum theory of aromatic hydrogen carcinogenisis, *Int. J. Quantum Chem: Quantum Biol. Symp*. **1974**, *No. 1,* 123-134.
50. Arieta, D. E.; Ontiveros, C. C.; Li, W-W.; Garcia, C. H.; Denison, M. S.; McDonald, J. D.; Burchiel, S. W.; Washburn, B. S.: Arylhydrocarbon receptor-mediated activity of particulate organic matter from the Paso del Norte airshed along the U.S.-Mexico border, *Environ. Health Perspectives*, **2003**, *111 (10),* 1299-1305.
51. Gerde, P.; Muggenburg, B. A.; Llundborg, M.; Dahl, A. R.: The rapid alveolar absorption of diesel soot adsorbed benzo[a]pyrene: bioavailability, metabolism and dosimetry of an inhaled particle-borne carcinogen, *Carcinogenisis*, **2001**, *22 4)*, 731-749.
52. Sato, H.; Sone, H.; Sagai, M.; Suzuki, K. T.; Yasunobu, A.: Increase in mutation frequency in lung of big blue rat by exposure to diesel exhaust, *Carcinogenisis*, **2000**, *21(4)*, 653-661.
53. Nikula, K. J.; snipes, M.B.; Barr, E. B.; Griffith, W. C.; Henderson, R. F.; Mauderly, J. L.: Comparative pulmonary toxicities and carcinogenicities of chronically inhaled diesel exhaust and black carbon in F344 rats, *Fund. Appl. Toxicol.* **1995**, *25(1)*, 80-94.
54. Heinrich, U.; Muhle, H.; Takenaka, S.; Ernst, E.; Fahst, R.; Mohr, U.; Pott, F.; Stöber, W.: Chronic effects on the respiratory tract of hamsters mice, and rats after long-term inhalation of high concentration of filtered and unfiltered diesel engine emissions, *J. Appl. Toxicol.* **1986**, *6*, 383-395.
55. Brightwell, J.; Fouillet, X.; Cassano-Zoppi, A.L.; Bernstein, D; Crawley, F.; Duchoustal, F.; Gatz, R.; Perezel, S.; Pfeifer, H.: tumors of the respiratory tract in rats and hamsters following chronic inhalation of engine exhaust emissions, *J. Appl. Toxicol.* **1998**, *9*, 23-31.
56. Heinrich, U.; Fahrst, R.; Rittinghausen, S.; Creutzenberg, O.; Belllman, B.; Koch, W.; Zessen, K.: Chronic inhalation exposure of Wistar rats an two different strains of mice to diesel engine exhaust, carbon black, and titanium dioxide, *Inhal. Toxicol* **1995**, *7(4)*, 533-556.
57. Wilson, M. R.; Lightbody, J. H.; Donaldson, K.; Sales, J.; Stone, V.: Interactions between ultrafine particles and transition metals *in vivo* and *in vitro*, *Toxicol. Appl. Pharmacol.* **2002**, *184(2)*, 172-179.
58. Carter, J. D., Ghio, A. J.; Samet, J. M.; Devlin, R. B.: Cytokine production by human airway epithelial cells after exposure to an air pollution particle is metal-dependent, *Toxicol. Appl. Pharmacol.* **1997**, *146(2)*, 180-188.
59. Salnikow, K.; Wecheng, S.; Blagosklanny, M.W.; Costa, M.: Carcinogenic metals induce hypoxia-inducible factor-stimulated transcription by reactive oxygen species-independent mechanism, *Cancer Res.* **2006**, *60*, 3375-3378.
60. Donaldson, K.; Tran, C. L.: Inflammation caused by particles and fibers, *Inhal. Toxicol.* **2002**, *14(1)*, 5-27.
61. Donaldson, K.; Stone, V.; Tran, C. L.; Kreyling, W.; Borm, P. J.: Nanotoxicology, *Occup. Environ. Med.* **2004**, *61(9)*, 727-728.
62. Oberdörster, G.; Oberdöster, E.; Oberdöster, J.: Nanotechnology: an emerging discipline evolving from studies of ultrafine particles, *Environ. Health Perspectives*, **2005**, *113*, 823-839.